

NMR on Anisotropic Magnetic Moment of Surface Bound States in Topological Superfluid $^3\text{He-B}$

M. Človečko, E. Gažo, M. Skyba, and P. Skyba*

Institute of Experimental Physics, SAS and P. J. Šafárik University Košice, Watsonova 47, 04001 Košice, Slovakia.

(Dated: September 6, 2018)

We present experimental observation of a new NMR effect on anisotropic magnetic moment of the surface Andreev-Majorana bound states in topological superfluid $^3\text{He-B}$ in zero temperature limit. We show that a formation of the anisotropic magnetic moment near the horizontal surface of a mechanical resonator, as a consequence of the symmetry violation of the superfluid $^3\text{He-B}$ order parameter by the resonator's surface and simultaneously modifying the excitation spectrum, may lead to anomalous damping of its mechanical motion in magnetic field. In difference to classical NMR technique, here NMR was excited using own harmonic motion of the mechanical resonator, and nuclear magnetic resonance was detected as a maximum in damping when resonator's angular frequency satisfied the Larmor resonance condition.

PACS numbers: 67.30.-n, 67.30.H-, 67.30.hj, 67.30.er, 67.80.D-, 67.80.dk

Superfluid phases of helium-3 provide one of the most complex and purest physical system to which we have access to, this is also a system that provides and serves as a model system for high energy physics, cosmology and quantum field theories. In fact, the phase transition into a superfluid state violates simultaneously three symmetries: the orbital, the spin and the gauge symmetry ($\text{SO}^L(3) \times \text{SO}^S(3) \times \text{U}(1)$) and created superfluid either A phase or B phase, resembles the physical features comparable with those in the Standard model or Dirac vacuum, respectively [1]. The symmetry of the superfluid condensate is also violated near any macroscopic or microscopic surface with which the superfluid phase of ^3He comes into contact. Presence of the surface enforces only the superfluid component that consists of the Cooper pairs having their orbital momenta oriented in direction to the surface normal and suppresses all others. This results in a distortion of the energy gap in direction of the surface normal on the distance of the order of a few coherence lengths ξ ($\xi \sim 100 \text{ nm}$) apart from the surface, and this gap distortion causes that superfluid surface layer of ^3He and fermionic excitations trapped in surface Andreev-Majorana bound (SAMB) states exhibit strong motional and magnetic anisotropy. It is worth to note that the dispersion relation of some of these excitations resembles the features of Majorana fermions, the fermions, which are their own antiparticles [2–5].

This article deals with experimental observations of nuclear magnetic resonance (NMR) performed on surface magnetic layer in superfluid $^3\text{He-B}$ at temperature of $175 \mu\text{K}$ and pressure of 0.1 bar. In contrast to application of the traditional NMR techniques, the magnetic resonance was achieved using an oscillating mechanical resonator in magnetic field and the absorption of the high frequency field by the spins in surface layer was detected as an additional magnetic field dependent mechanical damping of the resonator's motion.

In order to be able to study physical property of the

surface states, the superfluid $^3\text{He-B}$ has to be cooled to zero temperature limit. When superfluid $^3\text{He-B}$ is cooled below $250 \mu\text{K}$, the quasiparticle flux of the volume excitations falls with temperature as $\phi_V \sim D(p_F)T \exp(-\Delta/k_B T)$ due to presence of the energy gap Δ in the spectrum of excitations [6]. Here, $D(p_F)$ denotes the density of states on the Fermi level. On the other hand, the gap distortion in vicinity of the surface modifies the dispersion relation for the excitations trapped in SAMB states to "A-like" phase and corresponding flux of the surface excitations ϕ_S varies non-exponentially ($\phi_S \sim D_S(p_F)T^3$), where $D_S(p_F)$ is the density of states near surface which depends on the surface quality. Therefore, one may expect that in superfluid $^3\text{He-B}$ at higher temperatures $\phi_S < \phi_V$ (in a hydrodynamic regime), while at ultra low temperatures (in a ballistic regime) a state when $\phi_S > \phi_V$ can be achieved. This temperature transition can be detected using e. g. mechanical resonators as a decrease of their sensitivity to the collisions with volume excitations with temperature. It is obvious that this transition temperature depends on the resonator's mass, the area and quality of the resonator's surface which determines the density of the surface states [7–10].

There are variety of mechanical resonators being used as experimental tools to probe the physics of topological $^3\text{He-B}$ at zero temperature limit [11–14]. As the mechanical resonators we utilize tuning forks. These piezoelectric devices have become very popular experimental tools used in superfluid ^3He physics [15]. They are magnetic field insensitive, simply to install, easy to excite with extremely low dissipation of the order of a few fW or even less (and displacement $\sim 0.1 \text{ nm}$) and straight forward to measure the corresponding current I_F , which is proportional to the fork velocity $I_F = Av$, where A is the proportionality constant readily determined from experiment [16, 17].

The experiments were made in a double walled experi-

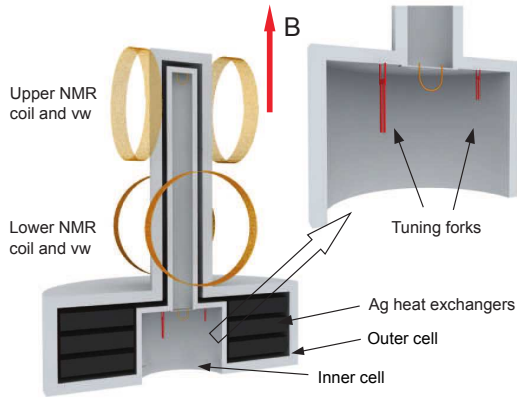


FIG. 1: (Color online) A schematic sketch of the double walled experimental cell mounted on our nuclear stage. The orientation of magnetic field B is shown as well.

mental cell mounted on a diffusion-welded copper nuclear stage (see Fig. 1) [18]. While upper tower served for NMR measurements (not mentioned here), in the lower part of the experimental cell, tuning forks of different sizes and one NbTi vibrating wire were mounted. The NbTi vibrating wire served as a thermometer in ballistic regime, in temperature range below $250\mu\text{K}$. After cooling the fridge down to $\sim 0.9\text{K}$, characteristics of the tuning forks in vacuum were measured in order to determine α constants for the individual forks. Both forks behaved as the high Q -resonators having Q -value of the order of 10^6 .

Figure 2 shows the width Δf_2 as a function of the fork velocity measured for the large and small tuning forks in superfluid $^3\text{He-B}$ at temperature of $175\mu\text{K}$ and pressure of 0.1bar . As one can see, there is a remarkable difference between them. The small tuning fork clearly demonstrates the Andreev reflection process [6, 19, 20]: as the fork velocity increases more and more volume excitations undergo the process of the Andreev reflection and being scattered, they exchange a tiny momentum with the fork of the order of $(\Delta/E_F)p_F$, E_F and p_F are the Fermi energy and the Fermi momentum, respectively. As a result, the fork damping decreases until a critical velocity is reached, when the fork motion begins to break the Cooper pairs and its damping rises again. However, this dependence for the large tuning fork is opposite: the damping of the large tuning fork increases with its velocity at the beginning. Different width Δf_2 - velocity dependence for the large fork presented in Fig. 2 suggests the presence of other dissipation mechanism than the Andreev reflection.

The reason for this assumption lies in difference between surface quality of the large and small fork: while the surface of the large fork is very diffusive, the surface of the small fork is much smoother (see Fig. 2).

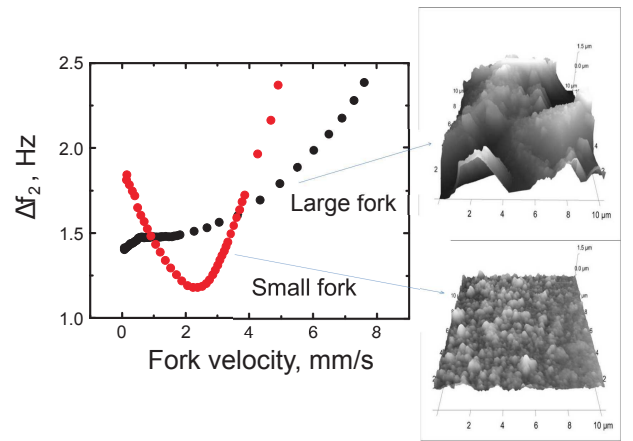


FIG. 2: (Color online) Dependence of the width Δf_2 for large (black) and small (red) tuning forks as a function of fork velocity and images of the surface profiles of tuning forks used in experiment obtained from AFM scans.

Having very diffusive surface, the large fork possesses much higher density of the SAMB states than that for the small fork. Therefore, we assume that at temperature $\sim 175\mu\text{K}$, density of excitations near the surface of the large fork satisfies condition $\phi_S > \phi_V$, while this condition is not valid for the small fork. However, at lower temperatures similar properties, as these measured with large fork, should be seen for small fork as well. When we measured the forks damping at temperature $175\mu\text{K}$, we surprisingly found that the damping of the large fork is magnetic field dependent and shows a maximum.

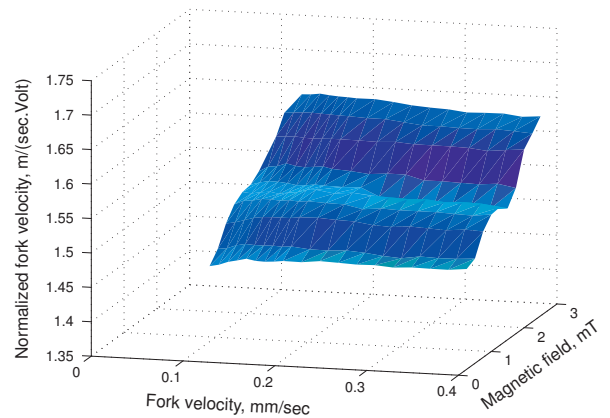


FIG. 3: (Color online) Dependence of the normalized tuning fork velocity (fork velocity over excitation voltage) as a function of the fork velocity and applied magnetic field B_0 . Dependence clearly shows a presence of the velocity minima at magnetic fields that satisfy the Larmor resonance condition $\omega_L = \gamma(B_0 + B_{rem})$.

Figure 3 shows dependence of the normalized tuning

fork velocity as a function of the fork velocity and magnetic field. This dependence is masked by a tiny thermal background due to a small warm-up caused by a parasitic heat leak into nuclear stage. When thermal background is subtracted off, the resulting dependencies are presented in Fig. 4.

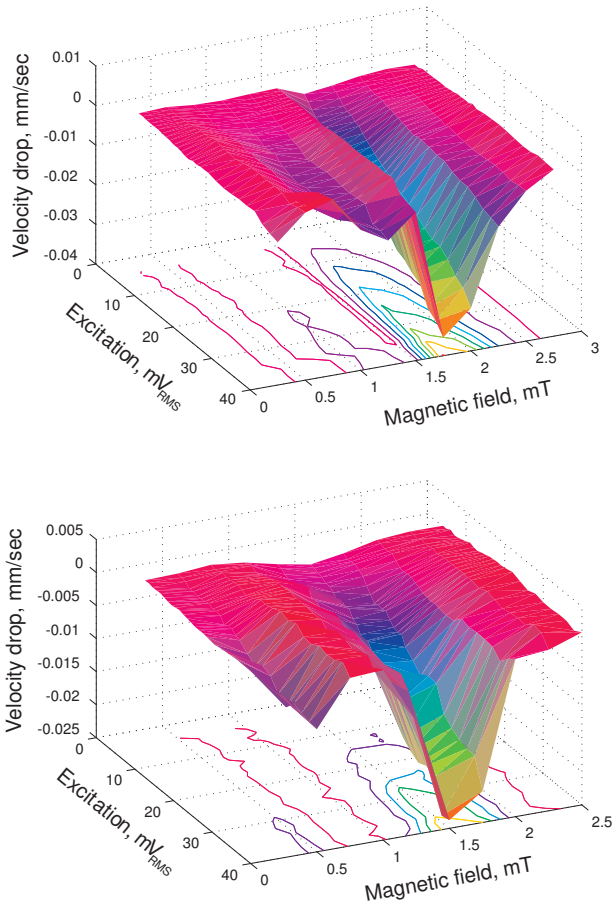


FIG. 4: (Color online) Two dependencies of the velocity drop of the tuning fork expressed as a function of the magnetic field B_0 and excitation voltage measured during two subsequent demagnetizations. Both dependencies show a clear minimum in velocity as function of the magnetic field at value that corresponds to the Larmor resonance frequency $\omega_F = \gamma(B_0 + B_{rem})$. We note that value of B_{rem} is ~ -0.5 mT.

Figure 4 manifests a new phenomenon: a presence of the velocity minima (i.e. an additional damping) at magnetic fields which satisfy the Larmor resonance condition $\omega = \gamma(B_0 + B_{rem}) = \gamma B$, where ω is the angular frequency of the tuning fork ($\omega \simeq 2\pi \cdot 32.4$ kHz), γ is the ^3He gyromagnetic ratio ($\gamma = -2\pi \cdot 32.4 \times 10^3$ rad/s.mT), B_0 and B_{rem} is the magnetic field applied and remnant magnetic field from demagnetization magnet, respectively. We interpret this phenomenon as NMR effect on the anisotropic magnetic moment \mathbf{M} formed on

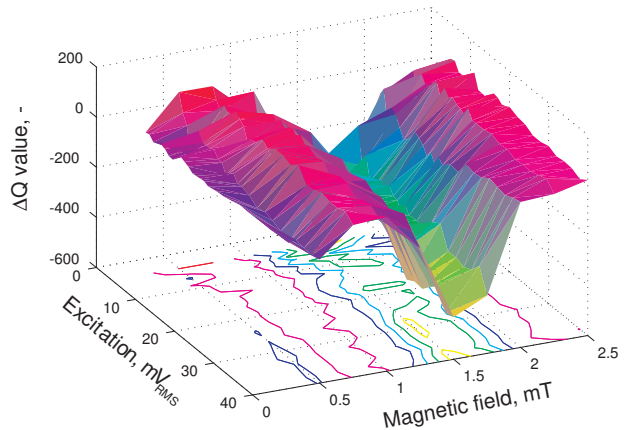


FIG. 5: (Color online) Dependence of the tuning fork Q-values as a function of magnetic field B_0 and excitation voltage. The deep minimum corresponds to nuclear magnetic resonance of the magnetic layer formed on tuning fork surface.

the horizontal surface of the tuning fork. Formation of the anisotropic magnetic moment \mathbf{M} is consequence of the symmetry violation of the $^3\text{He-B}$ order parameter by the fork surface, simultaneously modifying the excitation spectrum. At zero temperature limit, where measurements were performed, the influence of the SAMB states dominates, as the rest of superfluid $^3\text{He-B}$ in volume behaves like a vacuum. The magnetic moment \mathbf{M} of the surface layer includes the strong spin anisotropy of the superfluid ^3He layer, magnetic properties of the Andreev-Majorana bound fermionic excitations together with the solid ^3He atoms covering the fork's surface [10, 21]. Figure 5 shows the same NMR effect, however, as a drop of the tuning fork Q-value in dependence on the excitation and magnetic field.

In order to explain the measured dependencies we propose a simple phenomenological model as follows. The fork's motion in zero magnetic field can be described by the equation

$$\frac{d^2\alpha}{dt^2} + \Gamma \frac{d\alpha}{dt} + \omega_0\alpha = F_m \sin(\omega t), \quad (1)$$

where Γ is the damping coefficient characterizing the fork's interaction with surrounding superfluid $^3\text{He-B}$, ω_0 is the fork resonance frequency in vacuum, ω is the angular frequency of the external force, α is the deflection angle of the tuning fork arm from equilibrium and F_m is the force amplitude normalized by the mass m and by the length l of the tuning fork arm. We assume that fork's deflections are small enough and therefore interaction of the tuning fork with superfluid $^3\text{He-B}$ acts in linear regime i.e. we neglect processes of the Andreev reflection [6, 20]. By applying external magnetic field $\mathbf{B} = (0, 0, B_0 + B_{rem})$, the anisotropic magnetic mo-

ment $\mathbf{M}_0 = (0, 0, M_0)$ is formed on the fork's horizontal surfaces. When fork oscillates in external magnetic field \mathbf{B} , the normal to its horizontal surface \mathbf{m} is deflected from the direction of the external magnetic field \mathbf{B} . This means that anisotropic magnetic moment \mathbf{M} of the surface layer undergoes the same deflections (oscillations). Therefore, in the reference frame connected to the magnetic moment \mathbf{M} , this moment experiences a linearly polarized alternating magnetic field \mathbf{B}_{rf} of amplitude $B_{rf} = B \sin(\alpha) \simeq B\alpha$ oscillating with angular frequency ω of the tuning fork (see Fig. 6). While magnetic field magnitude in the direction of magnetic moment \mathbf{M} is $B_M = B \cos(\alpha) \simeq B$. Thus, a typical experimental NMR configuration is set up. However, here the excitation field \mathbf{B}_{rf} is "generated" by oscillating mechanical torque of the tuning fork. We suppose that magnetic torque $\mathbf{M} \times \mathbf{B}$ acting on the anisotropic magnetic moment \mathbf{M} is equivalent to the mechanical torque $\mathbf{L} \times \mathbf{F}_B$, where $\mathbf{L} = (L_x, 0, L_z)$ is the vector pointed in direction of \mathbf{M} having the magnitude equal to the length of the oscillating fork prong l . The force \mathbf{F}_B emerges from the rising of the Zeeman energy $(-\mathbf{M} \cdot \mathbf{B})$ due to deflection of \mathbf{M} from the field direction, acts against excitation force \mathbf{F}_m and causes additional field-dependent damping of the tuning fork motion. This force can be expressed as

$$\mathbf{F}_B = \frac{1}{\gamma l^2} \frac{d\mathbf{M}}{dt} \times \mathbf{L}. \quad (2)$$

In order to obtain time dependence of \mathbf{F}_B one has to determine dynamics of the magnetic moment \mathbf{M} which is governed by the Bloch's equation (in rotating reference frame)

$$\frac{\delta \mathbf{M}}{\delta t} = \gamma (\mathbf{M} \times \mathbf{B}_{eff}) + \frac{\mathbf{M}_0 - \mathbf{M}}{T_i}. \quad (3)$$

Here $\mathbf{M} = (M_x, M_y, M_z)$, $\mathbf{B}_{eff} = (-B_{rf}, 0, B - \omega/\gamma)$, and the second term on the right side describes the processes of the energy dissipation being characterized by the relaxation time constants T_i with $i = 1$ for z -component and $i = 2$ for xy -component of the magnetic moment \mathbf{M} . Assuming that magnetic relaxation processes act solely in the magnetic layer near fork surface and using the geometry of the problem, the amplitude of the force F_B acting against excitation force F_m can be expressed as

$$F_B = \frac{1}{\gamma l} \frac{dM_Y}{dt} = \frac{1}{\gamma l} [\chi_D \cos(\omega t) + \chi_A \sin(\omega t)] B \frac{d\alpha}{dt}, \quad (4)$$

where M_Y is the y -component of magnetic moment \mathbf{M} in the laboratory frame, ω is the tuning fork angular frequency, χ_A denotes the absorption component of the magnetic susceptibility of the layer expressed in the form

$$\chi_A = \frac{\chi_L \omega_B T_2}{1 + (\omega_B - \omega)^2 T_2^2} \quad (5)$$

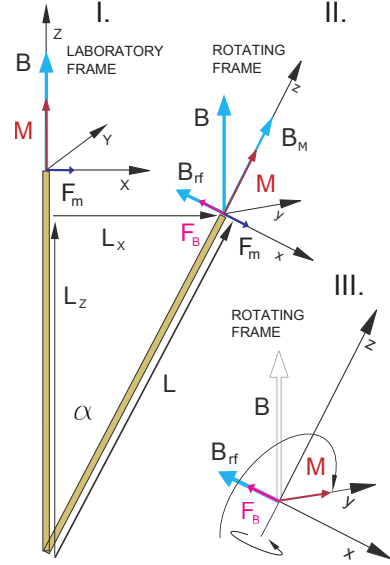


FIG. 6: (Color online) Schematic view on individual vectors for two positions of the tuning fork. In stationary position (I.) Zeeman energy is minimized and magnetic torque is zero. When fork is deflected by external force \mathbf{F}_m (II.), the rise of Zeeman energy due to anisotropy of the magnetic moment \mathbf{M} is associated with emergence of the force \mathbf{F}_B which acts against external force \mathbf{F}_m and causes additional, magnetic field dependent damping. When NMR condition is satisfied (III.) i.e. when $B_{eff} = B_{rf}$, magnetic moment \mathbf{M} precesses in $z - y$ plane around \mathbf{B}_{rf} in rotating frame of the reference.

and χ_D denotes the dispersion component in the form

$$\chi_D = \frac{\chi_L \omega_B (\omega_B - \omega) T_2^2}{1 + (\omega_B - \omega)^2 T_2^2}. \quad (6)$$

Here $\omega_B = \gamma B$ and $M = \chi_L B$, where χ_L stands for the magnetic susceptibility of the ^3He -layer. Adding the term (4) into equation (1), one gets nonlinear differential equation describing the tuning fork motion with anisotropic magnetic layer on its horizontal surface in external magnetic field in form

$$\frac{d^2\alpha}{dt^2} + \Gamma \frac{d\alpha}{dt} + \frac{1}{\gamma l^2 m} \frac{dM_Y}{dt} + \omega_0 \alpha = F_m \sin(\omega t). \quad (7)$$

Applying Runge-Kutta method we numerically calculated the time evolution of the tuning fork response described by the equation (7) as a function of applied external force (frequency and amplitude) and magnetic field. Calculated resonance characteristics were fitted using the Lorentz function in order to obtain experimentally measurable parameters: the velocity amplitude, the width and the resonance frequency as the function of the excitation and magnetic field. Figure 7 shows calculated dependencies of the tuning fork velocity difference as function of the excitation and magnetic field. The magnetic properties of surface layer were characterized by the spin-spin

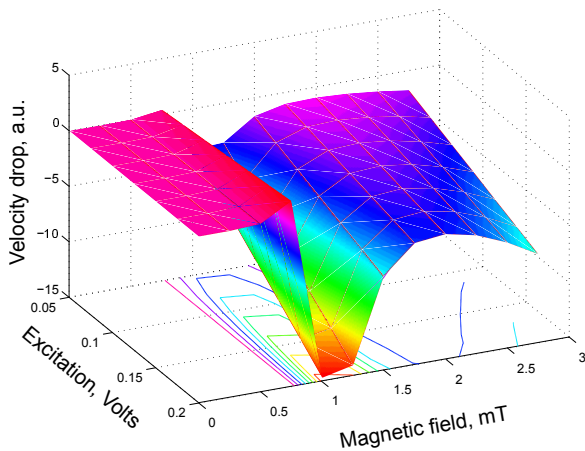


FIG. 7: (Color online) Theoretical dependence of the tuning fork velocity drop as a function of the magnetic field B_0 and excitation voltage calculated using equation (7).

relaxation time constant $T_2=28 \mu\text{sec}$. Presented dependencies are in very good qualitative agreement with those obtained experimentally and showed in Fig. 4.

Theoretical model presented in [10] suggests that this strong spin anisotropy of superfluid ^3He film near the surface is large enough to be observed experimentally. Perhaps, above mentioned technique of application of the mechanical resonators (e.g. tuning forks) with various surface roughness is a way. However, the open question is an influence of the solid helium-3 on this phenomenon, as the magnetic susceptibility of the solid helium-3 dominates at ultra low temperatures [21]. This could be tested by using ^4He as a coverage on the surface of the tuning fork, since ^4He atoms remove ^3He atoms from the surface. However, ^4He simultaneously covers the heat exchangers inside nuclear stage and this reduces the cooling efficiency of the ^3He liquid. As the measurements are performed in temperature range below $200 \mu\text{K}$, the test of influence of the ^3He solid layer on the observed phenomenon is going to be an experimental challenge.

In conclusion, we have observed the NMR effect on anisotropic magnetic moment of the superfluid surface layer, including Andreev-Majorana fermionic excitations and solid ^3He atoms, formed on the resonators' surface, being detected as additional magnetic field dependent damping of its mechanical motion. Further work is required to develop this technique, which in combination with non-standard NMR methods based on PPD [22] opens a possibility to study the spin dynamics of excitations trapped in SAMB states in topological superfluid $^3\text{He-B}$ and, perhaps, to prove their Majorana character.

We acknowledge the support of APVV-14-0605, VEGA 2/0157/14, Extrem II - ITMS 26220120047 and European Microkelvin Platform, H2020 project 824109. We wish to thank to M. Kupka for fruitful discussion and to Š. Bicaák

and G. Pristáš for technical support. Support provided by the U.S. Steel Košice s.r.o. is also very appreciated.

* Electronic Address: skyba@saske.sk

- [1] G. E. Volovik, *Universe in Helium-3 Droplet*, Clarendon Press, Oxford (2003).
- [2] Suk Bum Chung, Shou-Cheng Zhang, *Phys. Rev. Lett.* **103**, 235301 (2009).
- [3] S. Murakawa, Y. Tamura, Y. Wada, M. Wasai, M. Saitoh, Y. Aoki, R. Nomura, Y. Okuda, Y. Nagato, M. Yamamoto, S. Higashitani, and K. Naga, *Phys. Rev. Lett.* **103**, 155301 (2009).
- [4] G. E. Volovik, *JETP Lett.* **91**, 201 (2010).
- [5] T. Mizushima, K. Machida, *J. Low Temp. Phys.* **162** 204 (2011).
- [6] S. N. Fisher, A. M. Guénault, C. J. Kennedy, G. R. Pickett, *Phys. Rev. Lett.* **63**, 2566 (1989).
- [7] Y. Nagato, M. Yamamoto, K. Nagai, *J. Low Temp. Phys.* **110**, 1135 (1998).
- [8] A. B. Vorontsov, J. A. Sauls, *Phys. Rev. B* **68**, 064508 (2003).
- [9] Y. Aoki, Y. Wada, M. Saitoh, R. Nomura, Y. Okuda, Y. Nagato, M. Yamamoto, S. Higashitani, and K. Nagai, *Phys. Rev. Lett.* **95**, 075301 (2005).
- [10] Y. Nagato, S. Higashitani, K. Nagai, *J. of the Phys. Soc. of Japan* **78** 123603 (2009).
- [11] D. I. Bradley, P. Crookston, S. N. Fisher, A. Ganshin, A. M. Guénault, R. P. Haley, M. J. Jackson, G. R. Pickett, R. Schanen, V. Tsepelin, *J. Low Temp Phys* **157**, 476 (2009).
- [12] D. I. Bradley, S. N. Fisher, A. M. Guénault, R. P. Haley, R. C. Lawson, G. R. Pickett, R. Schanen, M. Skyba, V. Tsepelin, and D. E. Zmееv, *Nature Physics*, **12**, 1017 (2016).
- [13] P. Zheng, W. G. Jiang, C. S. Barquist, Y. Lee, and H. B. Chan, *Phys. Rev. Lett.* **117**, 195301 (2016).
- [14] P. Zheng, W. G. Jiang, C. S. Barquist, Y. Lee, and H. B. Chan, *Phys. Rev. Lett.* **118**, 065301 (2017).
- [15] R. Blaauwgeers, M. Blažková, M. Človečko, V. B. Eltsov, R. de Graaf, J. Hosio, M. Krusius, D. Schmoranzler, W. Schoepe, L. Skrbek, P. Skyba, R. E. Solntsev, D. E. Zmееv, *J. Low Temp. Phys.* **146**, 537 (2007).
- [16] P. Skyba, *J. Low Temp. Phys.* **160**, 219 (2010).
- [17] S. Holt, P. Skyba, *Rev. Sci. Instrum.* **83**, 064703 (2012).
- [18] P. Skyba, J. Nyéki, E. Gažo, V. Makróczyová, Yu. M. Bunkov, D. A. Sergackov, A. Feher, *Cryogenics* **37**, 293 (1997).
- [19] D. I. Bradley, M. Človečko, E. Gažo, P. Skyba, *J. Low Temp. Phys.* **152**, 147 (2008), DOI:10.1007/s10909-008-9815-5.
- [20] M. Človečko, E. Gažo, M. Kupka, M. Skyba, P. Skyba, *J. Low Temp. Phys.* **162** 669 (2011), DOI 10.1007/s10909-010-0330-0.
- [21] D. I. Bradley, S. N. Fisher, A. M. Guénault, R. P. Haley, N. Mulders, G. R. Pickett, D. Potts, P. Skyba, J. Smith, V. Tsepelin, and R. C. V. Whitehead, *Phys. Rev. Lett.* **105**, 125303 (2010).
- [22] S. N. Fisher, G. R. Pickett, P. Skyba, and N. Suramlishvili, *Phys. Rev. B* **86**, 024506 (2012).